Experimental and Modeling Study on Decomposition Kinetics of Methane Hydrates in Different Media

ARTICLE *in* THE JOURNAL OF PHYSICAL CHEMISTRY B · NOVEMBER 2005

Impact Factor: 3.3 · DOI: 10.1021/jp0526851 · Source: PubMed

6 AUTHORS, INCLUDING:

Chang-Yu Sun
China University of Petroleum
107 PUBLICATIONS **1,279** CITATIONS

SEE PROFILE

Experimental and Modeling Study on Decomposition Kinetics of Methane Hydrates in Different Media

Minyan Liang, Guangjin Chen,* Changyu Sun, Lijun Yan, Jiang Liu, and Qinglan Ma

State Key Laboratory of Heveay Oil Processing, Chinese University of Petroleum, Changping County, Beijing 102249, People's Republic of China

Received: May 22, 2005; In Final Form: August 20, 2005

The decomposition kinetic behaviors of methane hydrates formed in 5 cm^3 porous wet activated carbon were studied experimentally in a closed system in the temperature range of 275.8−264.4 K. The decomposition rates of methane hydrates formed from 5 cm^3 of pure free water and an aqueous solution of 650 $g \cdot m^{-3}$ sodium dodecyl sulfate (SDS) were also measured for comparison. The decomposition rates of methane hydrates in seven different cases were compared. The results showed that the methane hydrates dissociate more rapidly in porous activated carbon than in free systems. A mathematical model was developed for describing the decomposition kinetic behavior of methane hydrates below ice point based on an ice-shielding mechanism in which a porous ice layer was assumed to be formed during the decomposition of hydrate, and the diffusion of methane molecules through it was assumed to be one of the control steps. The parameters of the model were determined by correlating the decomposition rate data, and the activation energies were further determined with respect to three different media. The model was found to well describe the decomposition kinetic behavior of methane hydrate in different media.

1. Introduction

Gas hydrates are crystalline compounds formed from water (the host species) and small gas molecules (the guest species). There are three known hydrate structures: structure I, structure II,[1−3] and structure H.[4] Methane forms structure I hydrate in usual cases.

Gas hydrate has been viewed as a gas storage media as it can contain up to 180 volumes (at standard temperature and pressure) of methane gas per volume of hydrate in theory. The storage of natural gas in the form of hydrate (NGH) is appealing for industrial utilization because of not only its high storage capacity, but also the storage safety resulting from its higher stability at atmospheric pressure and not very low temperature. Gudmundsson et al.[5] demonstrated that natural gas hydrate could be stored at the temperature above 258 K at atmospheric pressure for a long time. Recently, Yan et al.[6] studied the formation of methane hydrate in wet activated carbon. They found that the storage capacity and the formation rate of hydrate could be dramatically enhanced by immersing activated carbon in water. The advantages of the storage of natural gas in wet activated carbon have also been demonstrated by other researchers,[7−9] but the decomposition characteristics of methane hydrates formed in wet activated carbon have not been studied so far.

Additionally, large quantities of natural gas hydrates have been found in the permafrost region and deep oceans. It is estimated that the total amount of carbon in hydrate form is twice that of all conventional resources (coal, oil, natural gas) combined.[10] Therefore, it is meaningful to study the decomposition kinetics of hydrates for both the storage of natural gas and the exploitation of natural gas hydrate resources in situ.

In most studies on the decomposition kinetics of hydrate carried out so far, hydrates were formed in the bulk free water. Kim et al.[11] carried out experiments on methane hydrates decomposition at temperature from 274 to 283 K and pressures from 0.17 to 6.97 MPa in a stirring reactor. They also developed a kinetic model for the intrinsic rate of gas hydrate decomposition and determined the rate constant from experimental data for methane. Clarke and Bishnoi[12−14] determined the intrinsic decomposition rates of ethane hydrate, methane hydrate, and methane-ethane binary hydrate, respectively, by measuring the decomposition rates in a stirring reactor above ice point. Stern et al.[15] and Shirota et al.[16] performed methane hydrate decomposition experiments below the ice point. It was demonstrated that the decomposition rate of hydrate did not decrease monotonically with the decrease of temperature in Stern et al.'s work. Lin et al.[17] investigated the effects of the anionic surfactant sodium dodecyl sulfate (SDS), which has been proven to be a very good kinetic promoter enhancing hydrate formation on the decomposition kinetic behaviors of methane hydrate, especially on those below the ice point. It was demonstrated that the presence of SDS lowered the stability of hydrate.

Because gas hydrates in nature largely exist in porous media, the research on the hydrates in porous media is very important for the exploitation of natural gas hydrate resources. Several studies on gas hydrate in porous media have been reported,[9,18−19] but most of them concentrated on the phase equilibrium of gas hydrates, and few were on the decomposition kinetics of hydrates.

In the present work, the decomposition kinetic behavior of methane hydrates formed in the porous activated carbon is investigated and compared with that of hydrate formed in pure free water or aqueous solution of SDS. A mathematical model is developed to describe the decomposition kinetics of methane hydrate in different media.

2. Experimental Section

2.1. Equipment and Material. A schematic of the experimental apparatus is shown in Figure 1. The critical part of the

* Corresponding author. E-mail address: gjchen@cup.edu.cn.

10.1021/jp0526851 CCC: $30.25
Published on Web 09/20/2005

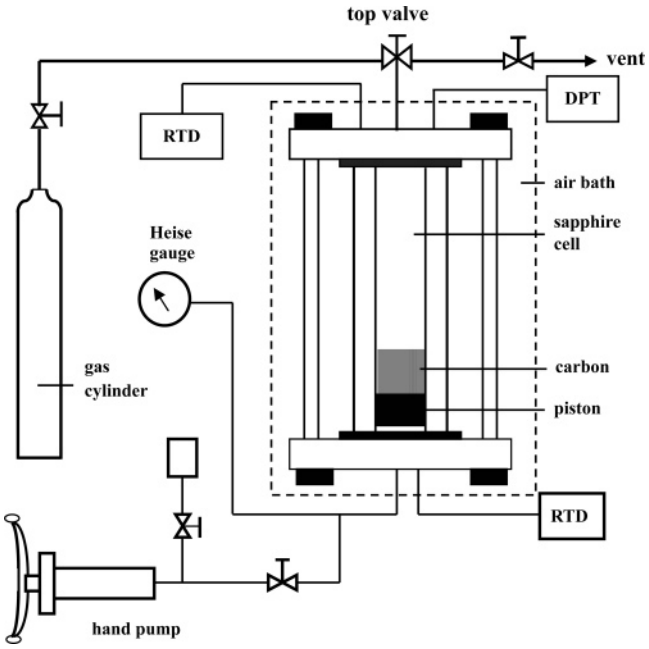

Figure 1. Experimental apparatus for studying hydrate formation/decomposition phenomenon.

apparatus is a transparent sapphire cell with a diameter of 2.54 cm through which the formation/decomposition process of the hydrate can be observed directly. The maximum workspace of the cell is 78 cm^3, whereas the designed maximum working pressure is 20 MPa. The volume of the system can be altered by moving the piston up or down with a hand pump. The change of volume can be read from the scale of the pump with a precision of 0.002 mL. To observe the experimental phenomena occurring in the cell clearly, a luminescence source of type LG100H is fixed on the outside of the cell. The system temperature is controlled by an air bath with a precision of 0.1 K. The temperature sensor used is a secondary platinum resistance thermometer (type pt100). A calibrated Heise pressure gauge and differential pressure transducers are used to measure the system pressure. The uncertainties of pressure and temperature measurements are ±0.01 MPa and ±0.1 K, respectively. The changes of the system temperature and pressure with time are recorded and displayed by a computer. One of the advantages of the apparatus is that the sapphire cell can be dismounted conveniently, which makes it suitable for the present experimental work. The apparatus was described in detail in the previous papers published by this laboratory.[6]

Analytical grade methane (99.99%) was obtained from Beifen Gas Industry Corporation. Activated carbon (particulate, analytical reagent) with a mesh number of 20−40 was purchased from the Dali Activated Carbon Plant in Beijing. The bulk density of activated carbon is 0.46 $g{\cdot}cm^{-3}$ and its specific surface area is 1126 $m^2{\cdot}g^{-1}$. The mean pore diameter of the activated carbon used in this work was measured to be 1.9 nm. Double-distilled water was used in all experiments, which was weighed by an analytical balance with a precision of 0.1 mg.

2.2. Experimental Method and Procedure. *2.2.1. Preparation of Hydrate Sample in Activated Carbon.* Before beginning the experiments, the sapphire cell was dismounted from the apparatus, washed with distilled water, and dried. It was then loaded with a known quantity of dry activated carbon, which was weighed precisely by using a balance with a precision of 0.1 mg. Subsequently, a known amount of distilled water was immersed into the activated carbon slowly and evenly. The mass of the immersed water was also weighed by the balance. The volume of the wet activated carbon was obtained by measuring the height of the wet carbon bed (the radius of cell is known to be 1.27 cm). After that, the cell was installed into the apparatus again. The system was evacuated for about half an hour, and the gas space of the system was then purged with methane 4−5 times to ensure the absence of air.

The temperature of the air bath was then adjusted to the desired value at which the hydrate sample was formed. Once the temperature of the system was kept constant, methane gas was charged into the cell until the system pressure reached the given value. When hydrates began to form, the pressure was decreased gradually. The pressure change in the cell with time was observed and recorded. When the drop in system pressure was less than 0.01 MPa over 3 h, the formation of hydrate sample was assumed to be complete. Additional details regarding the formation of hydrate in wet activated carbon can be found in our previous work.[6]

2.2.2. Hydrate Decomposition Test. The hydrate decomposition test began after the formation of a hydrate sample in the activated carbon. At first, the temperature of the air bath was adjusted to the desired value at which the hydrate decomposition test would be carried out. When the system was cooled to the desired temperature, the system was left for about 4 h with a fluctuation of temperature less than 0.1 K. Considering the radius of the cell, which is only 1.27 cm, 4 h was assumed to be long enough for the hydrate sample to reach equilibrium. Afterward, the vent of the cell was opened little by little and the system pressure was declined gradually until it reached somewhat above the equilibrium pressure of methane hydrate at the present temperature. Subsequently, the system was depressurized very rapidly to the atmospheric pressure and closed from the outside. Soon after that, the change of system pressure with the elapsed time was recorded. The temperature and total volume of the system were kept constant during the test. When the decomposition test was completed, the system was heated to make the residual hydrate decompose completely.

The cumulative moles of methane dissociated at time t were calculated from the following equation:

$$n = \frac{PV}{ZRT} - \frac{P_0 V}{RT} \tag{1}$$

where P is the system pressure at time t; P_0 is the initial decomposition pressure, which equals 0.1 MPa; T is the temperature; V is the volume of the gas space in the cell, which was specified to be a constant for all tests. The compressibility factor Z was calculated with the Benedict−Webb−Rubin equation of state.

3. Modeling of Hydrates Decomposition Kinetics below the Ice Point

Kim et al.[11] proposed a two-step mechanism for gas hydrate decomposition above ice point:

(1) Destruction of the clathrate host lattice at the surface of a hydrate particle.

(2) Desorption of the guest molecule (methane) from the surface of hydrate.

With these assumptions, the rate of hydrates decomposition was formulated as

$$\frac{dn_d}{dt} = k_d A_s (f_e - f_s) \tag{2}$$

where n_d is the cumulative moles of gas released at time t, A_s is the total surface area of the decomposing hydrate particles,

k_d is the decomposition rate constant. f_e and f_s represent the fugacity of methane at the water−hydrate−vapor three-phase equilibrium pressure and the fugacity of methane at the surface of the hydrate particle, respectively.

The decomposition kinetic behavior of hydrate below ice point in a static system is largely different from that above ice point. Anomalous preservation or self-preservation phenomenon that gas hydrates are of unexpected stability when they are brought outside their field of stability at temperature below ice point has been observed for decades.[5,20,21] However, more recently, Stern et al.[15,22−24] and Kuhs et al.[25] found that the effect also had a lower limit. According to Stern et al., the "anomalous preservation window" ranged from 240 K to the ice point, while at temperatures below 240 K, the decomposition was rapid and appeared to be thermally activated; within this window, the decomposition rates did not vary with temperature monotonically, and two minima existed at around 250 and 268 K. The in situ neutron diffraction experiments conducted by Kuhs et al. revealed that the low-temperature onset of the anomalous preservation coincided with the annealing of stacking faults of the ice formed initially; the defective, stacking-faulty ice below 240 K apparently did not present an appreciable diffusion barrier for gas molecules, while the annealed ordinary ice above this temperature clearly hindered gas diffusion.[25] Although the anomalous preservation phenomenon has been well-known, the mechanism for it still remains problematic. The ice-shielding mechanism seems to be a sound illustration of this phenomenon in which an ice layer surrounding the hydrate core is assumed to be formed after the initial dissociation stage and thickened with the proceeding of hydrates decomposition; the thickening ice layer hinders the hydrate from further decomposition, and the diffusion of methane molecules through it is the rate-determining step.[20] By using time-resolved X-ray diffraction techniques, Takeya et al.[26] confirmed the formation of ice Ih layer surrounding the hydrate particles and proposed a decomposition model based on the ice-shielding mechanism. More recently, as stated above, the in situ neutron diffraction experiments conducted by Kuhs et al. also supported this type of mechanism to some extent, and a model similar to that of Takeya et al. was developed by them.[25,27] The molecular dynamic simulation on the decomposition of Xe hydrate conducted by Tse and Klug supported the ice-shielding mechanism, too.[28] Additionally, in their comments on the work of Stern et al.,[15] Wilder and Smith[29] suggested a series of possible interpretations of the anomalous preservation, including the ice-shielding mechanism. On the other hand, this type of mechanism was refuted by Stern et al.[15,22−24] At first, they thought the ice-shielding mechanism could not explain the complex and extremely nonlinear temperature dependence of methane hydrate dissociation behavior. Second, by scanning electron microscopy, they observed the absence of ice rind development in preserved samples. Third, by evaluating the strain rate of ice rind in the anomalous preservation regime, they found it was mechanically impossible for a thin skin of ice (about 4 μm) to sustain an internal methane pressure of, for example, approximately 2 MPa at 270 K. Additionally, the lack of preservation observed by them in sII methane-ethane hydrate also supported their arguments.[22] Nevertheless, they agreed that the ice product did play some role in retarding hydrate dissociation.[30] We think that, although the further investigation into the mechanism for the anomalous preservation of methane hydrate is necessary, the ice-shielding mechanism could image the role of ice in hindering hydrate dissociation to some extent. Therefore, our modeling work is still based on the ice-shielding mechanism. In our arguments, the ice rind is not separated from the hydrate core, but linked tightly to it through hydrogen bonds. There also is not a separated gas phase between ice rind and hydrate core. Alternatively, the ice boundary contacting the hydrate core is saturated by the released gas molecules and supplies a gas fugacity higher enough to stabilize the inner hydrate as argued by Stern et al.[22−24] and Kuhs et al.[25] If this is the case, there is not the problem of whether the ice rind could sustain an internal methane pressure. The degree of perfection of ice might be the determining factor in limiting the decomposition rate, and perhaps, it is the nonlinear temperature dependence of the degree of perfection of ice that leads to the nonlinear temperature dependence of methane hydrate dissociation behavior in an anomalous regime. The temperature dependence of the degree of perfection of ice has been proven experimentally by Kuhs et al.[25]

According to the ice-shielding mechanism, the kinetic process of the hydrate decomposition in a static system below the ice point could be assumed as following two sequential steps:

(1) Destruction of the clathrate host lattice at the surface of a hydrate particle and desorption of the methane molecule from the surface of hydrate particle.

(2) Diffusion of the methane molecule through a porous (defective) ice layer and being released to vapor phase.

The first step was put forward in the work of Kim et al.[11] and could be described by eq 2. In the second step, we assumed that the fugacity of gas varies linearly in the direction of thickness of the porous ice layer mentioned above, so the diffusion rate of gas was formulated as:

$$\frac{dn_d}{dt} = \frac{D}{L}A_s(f_s - f_g) \tag{3}$$

where D denotes the diffusion coefficient of the gas molecule in a porous ice layer, L is the thickness of the porous ice layer, and f_g is the fugacity of methane in vapor phase.

The decomposition of hydrate was further assumed to be a quasistable process, i.e., the releasing rate of methane gas in surface decomposition reaction is equal to the diffusion rate of the methane molecule through the porous ice layer. Subsequently, by combining eq 2 and eq 3, the following equation was obtained,

$$k_d A_s(f_e - f_s) = \frac{D}{L}A_s(f_s - f_g) \tag{4}$$

By eliminating f_s in eq 4, the decomposition rate of hydrate below the ice point in a static system was then written as:

$$\frac{dn_d}{dt} = \left[\frac{1}{\frac{1}{k_d A_s} + \frac{L}{DA_s}}\right](f_e - f_g) \tag{5}$$

where L, the thickness of the porous ice layer, is the function of the quantity of hydrate decomposed, i.e., the function of n_d. The relation between L and n_d is very complex and should be characterized by the geometric form of the hydrate particle. Similarly, diffusion coefficient D should also be the function of n_d. In the beginning stage, the ice layer might not be closed and D should be very large; with the proceeding of hydrate decomposition, D will decrease. Both the increase of L and the decrease of D lead to the increase of diffusion resistance term L/DA_s in eq 5. The following empirical equation is used to formulate the relation between this term and n_d in this work,

$$L/DA_s = n_d^b/D_s \quad (6)$$

where b and D_s are empirical constants that can be determined from the experimental data. Therefore, eq 5 can be rewritten as

$$\frac{dn_d}{dt} = \left[\frac{1}{\frac{1}{K} + \frac{n_d^b}{D_s}}\right](f_e - f_g) \quad (7)$$

where $K = k_d A_s$.

4. Results and Discussion

4.1. Experimental Results. To ensure that the decomposition experiments are performed on the same basis, the temperature, initial pressure, the volume of gas space, the mass of the activated carbon, and the mass of water were uniformly specified to 276.5 K, 8 MPa, 71 cm^3, 2.3 g, and 3.3 g, respectively, when preparing the hydrate sample in activated carbon. The volume of hydrate sample (hydrate + activated carbon) formed at these conditions was 5 cm^3. The decomposition experiments were performed at five different temperatures ranging from 264.4 to 275.8 K with the initial decomposition pressures fixed at 0.1 MPa and the volumes of the methane gas fixed at 71 cm^3. The measured dissociation pressure profiles are depicted in Figure 2. By using eq 1, the cumulative moles of methane dissociated at different times were determined and are depicted in Figure 3, in which the calculated results by using the kinetic model developed in this work, i.e., eq 7, are also plotted for comparison. From Figure 2, it was observed that the hydrate decomposed rapidly above the ice point. The hydrate sample decomposed thoroughly in half an hour at 275.8 K; in 2 h at 273.2 K, no self-preservation was found. Because a small quantity of gas was lost during the depressurization process at 275.8 K, the final dissociation pressure at this temperature was lower than that at 273.2 K. Similar to the case above the ice point, hydrate also decomposed rapidly in the beginning stage. However, the dissociation rate decreased rapidly because of the self-preservation effect. The decomposition rate decreased with the decrease of the temperature monotonically. The minimum dissociation rate in the temperature range of 264−270 K reported by Stern et al.[15] was not observed in the dissociation of hydrate in activated carbon.

We have investigated the decomposition kinetic behavior of methane hydrates formed from 10 cm^3 pure free water or 10 cm^3 sodium dodecyl sulfate (SDS) aqueous solution below the ice point systematically in our former work.[17] For comparison, decomposition rates of methane hydrates formed from 5 cm^3 pure free water or 5 cm^3 sodium dodecyl sulfate (SDS) aqueous solution below the ice point were also measured in the current work; these results are shown in Figure 4 and Figure 5, respectively. It is interesting to find in Figure 4 that hydrate dissociated much more rapidly at 264.4 K than at 267.4 K for the hydrate formed from 5 cm^3 pure free water. It seems that no self-preservation effect existed at 264.4 K. This phenomenon was also reported by Stern et al.[15] However, as shown in Figure 5, this abnormal phenomenon was not found in the dissociation of hydrate formed from 5 cm^3 water with 650 $g \cdot m^{-3}$ SDS; the dissociation rate decreased monotonically with the decrease of temperature. This phenomenon also was not observed in the dissociation tests of hydrate formed from 10 cm^3 pure water or 10 cm^3 water with SDS in our former work.[17] Generally, our results are more in agreement with those reported by Shirota et al.[16] For a better comparison, the dissociation percentage profiles of methane hydrate in seven different cases at 267.4 and 264.4 K are depicted in Figure 6 and Figure 7, respectively. Except for the abnormal case stated above, methane hydrate dissociated fastest in activated carbon. As expected, hydrate with a larger

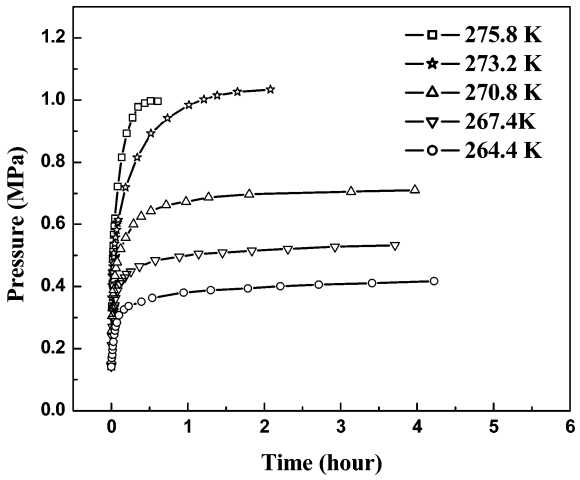

Figure 2. Dissociation pressure profiles of methane hydrate formed in activated carbon at different temperatures.

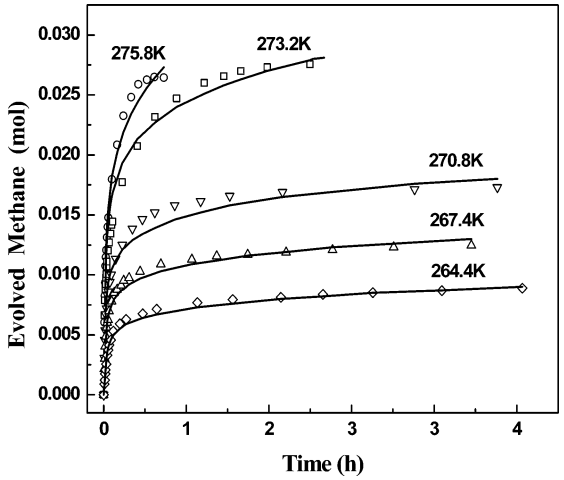

Figure 3. Cumulative moles of methane evolved at different times during the dissociation of methane hydrate formed from 5 cm^3 wet activated carbon (2.3 g carbon + 3.3 g water) at different temperatures. The open symbols represent the experimental data, whereas the solid curves are calculated from the developed model, eq 7.

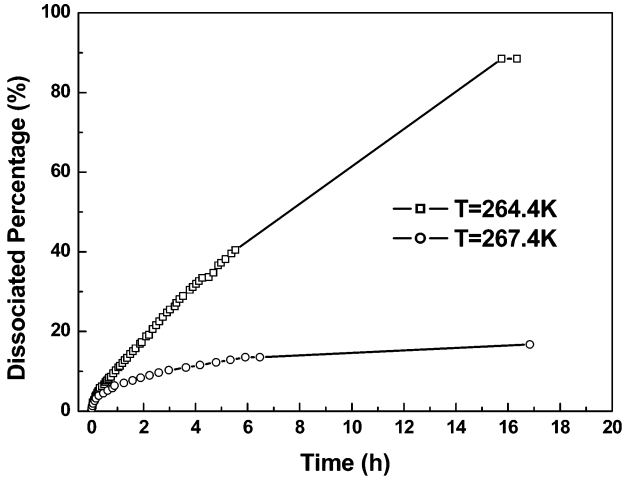

Figure 4. Dissociation percentage profiles of methane hydrate formed from 5 cm^3 water, where dissociation tests were carried out in a constant volume of 65 cm^3.

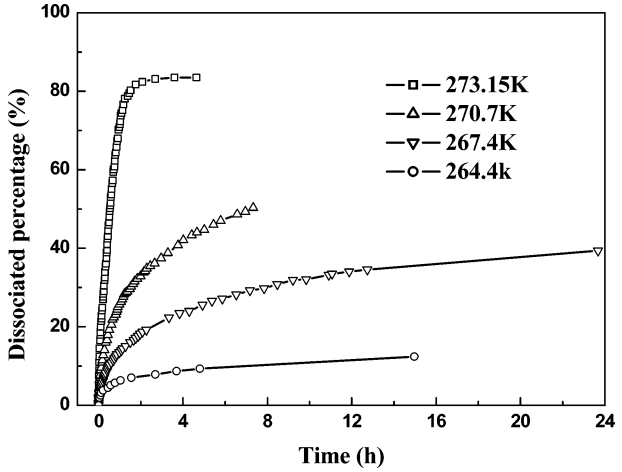

Figure 5. Dissociation percentage profiles of methane hydrate formed in 5 cm^3 water with 650 $g \cdot m^{-3}$ SDS, where all dissociation tests were carried out in a constant volume of 65 cm^3.

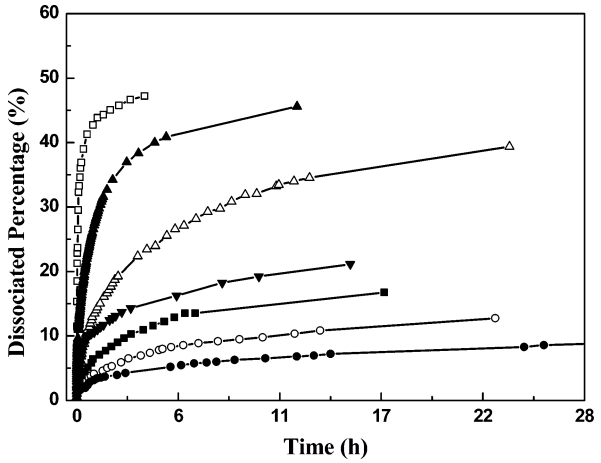

Figure 6. Dissociation percentage profiles of methane hydrate at 267.4 K with respect to seven different cases: (□) hydrate formed in 5 cm^3 wet activated carbon and dissociated in a constant volume of 76 cm^3; (▲) hydrate formed from 10 cm^3 water with 650 $g \cdot m^{-3}$ SDS and dissociated at atmospheric pressure;[17] (△) hydrate formed from 5 cm^3 water with 650 $g \cdot m^{-3}$ SDS and dissociated in a constant volume of 65 cm^3; (▼) hydrate formed from 10 cm^3 pure water and dissociated at atmospheric pressure;[17] (■) hydrate formed from 5 cm^3 pure water and dissociated in a constant volume of 65 cm^3; (○) hydrate formed from 10 cm^3 water with 650 $g \cdot m^{-3}$ SDS in a constant volume of 65 cm^3;[17] (●) hydrate formed from 10 cm^3 pure water and dissociated in a constant volume of 65 cm^3.[17]

volume dissociated more slowly than that with a smaller volume; hydrate dissociated more slowly in a closed system, i.e., with a constant volume, than in an open system that was connected with the atmosphere. The presence of SDS lowered the stability of hydrate.

4.2. Correlating of Experimental Data. The developed decomposition kinetic model formulated by eq 7 was used to correlate the measured experimental data, where the fugacity of methane, f_g or f_e, was calculated using the Peng−Robinson (PR) equation of state.[31] The vapor−water (or ice)−hydrate three-phase equilibrium pressures in free water systems required for calculating f_e were taken from the literature.[32] The presence of 650 $g \cdot m^{-3}$ SDS in water was assumed to be of no influence upon the formation condition of methane hydrate thermodynamically. The three-phase equilibrium pressures in activated carbon at experimental temperatures should be higher than those in a free water system and difficult to measure below the ice point because of self-preservation. Zanota et al.[9] recently

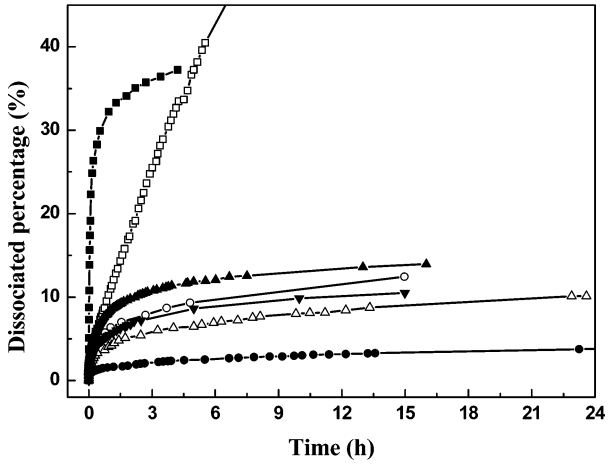

Figure 7. Dissociation percentage profiles of methane hydrate at 264.4 K with respect to seven different cases: (■) hydrate formed in 5 cm^3 wet activated carbon and dissociated in a constant volume of 76 cm^3; (□) hydrate formed from 5 cm^3 pure water and dissociated in a constant volume of 65 cm^3; (▲) hydrate formed from 10 cm^3 water with 650 $g \cdot m^{-3}$ SDS and dissociated at atmospheric pressure;[17] (○) hydrate formed from 5 cm^3 water with 650 $g \cdot m^{-3}$ SDS and dissociated in a constant volume of 65 cm^3; (▼) hydrate formed from 10 cm^3 pure water and dissociated at atmospheric pressure;[17] (△) hydrate formed from 10 cm^3 water with 650 $g \cdot m^{-3}$ SDS and dissociated in a constant volume of 65 cm^3;[17] (●) hydrate formed from 10 cm^3 pure water and dissociated in a constant volume of 65 cm^3.[17]

measured the equilibrium formation pressure of methane hydrate in wet activated carbon and found that the formation pressure at 274.2 K was 4.5 MPa, which corresponds to an equilibrium temperature in a bulk condition of 277.7 K or so. The activated carbon used by them, with a mesoporous diameter range from 3.5 to 4.5 nm, microporous diameter smaller than 0.8 nm, and a specific surface area of 1203 $m^2 \cdot g^{-1}$, is comparatable with the activated carbon used in this work, with an average pore diameter of 1.8 nm and a specific surface area of 1126 $m^2 \cdot g^{-1}$. It is a coincidence that the equilibrium formation pressure of methane hydrate at 274.2 K in a silica gel pore with a diameter of 14 nm, measured by Handa and Stupin,[19] was 4.6 MPa, which was very close to 4.5 MPa. Additionally, as shown in our previous work,[6] the methane hydrate formation pressures in the wet activated carbon used in the present work above ice point were also coincident with those in the 18-nm silica gel pore. Considering these coincidences, we took the hydrate formation pressures in the 14-nm silica gel pore as the three-phase equilibrium pressures in the wet activated carbon for the calculation of f_e. One may be curious about the formation of hydrate in a pore of the size of only 1.8 nm as the thermodynamic critical size of a stable hydrate nucleus is estimated to be 8−11 nm.[33] The reason should be mainly attributed to the fact that the water in the pores is not isolated, but connected with the water film on the surface of the carbon particle. The hydrate may form first from the water film, then grow inside the pores. Not only the pore diameter, but also the thickness of the water film, influences the shift of the hydrate formation conditions from those in bulk water.[34] This might be the reason the hydrate formation conditions in wet activated carbon with average pore size of 1.8 nm are consistent with those in 18-nm silica gel pore.

The values of three parameters, K, b, and D_s, in eq 7 were determined by fitting the decomposition rate data measured at fixed temperatures and tabulated in Tables 1−3, respectively, corresponding to three different media from which hydrates were formed, 5 cm^3 wet activated carbon, 10 cm^3 pure free water,

TABLE 1: Model Parameters in eq 7 with Respect to the Dissociation of Methane Hydrate Formed in 5 cm³ Wet Activated Carbon

T/K	P_e/MPa	f_e/MPa	$K' \times 10^5$/ mol·MPa^{-1}·s^{-1}·g^{-1}	b	$D_s \times 10^{15}$/ mol^{b+1}·MPa^{-1}·s^{-1}
275.8	5.071	4.592	1.439	4.458	73.795
273.2	4.347	3.964	1.310	5.849	0.1483
270.8	3.735	3.443	1.050	6.569	2.479×10^{-4}
267.4	3.09	2.892	0.681	7.050	2.617×10^{-6}
264.4	2.726	2.558	0.403	6.320	4.577×10^{-6}

TABLE 2: Model Parameters in eq 7 with Respect to the Dissociation of Methane Hydrate Formed from 10 cm³ Free Pure Water

T/K	f_e/MPa	$K' \times 10^7$/ mol·MPa^{-1}·s^{-1}·g^{-1}	b	$D_s \times 10^{10}$/ mol^{b+1}·m^{-1}·MPa^{-1}·s^{-1}
269.4	2.151	4.597	1.00	36.780
268.4	2.086	3.870	1.35	0.564
266.4	1.959	2.766	1.99	4.633×10^{-3}
264.4	1.840	2.044	2.32	1.297×10^{-4}

TABLE 3: Model Parameters in eq 7 with Respect to the Dissociation of Methane Hydrate Formed from 10 cm³ Free Water with the Presence of 650 g·m^{-3} SDS

T/K	f_e/MPa	$K' \times 10^7$/ mol·MPa^{-1}·s^{-1}·g^{-1}	b	$D_s \times 10^{10}$/ mol^{b+1}·m^{-1}·MPa^{-1}·s^{-1}
269.4	2.151	9.369	1.00	51.94
268.4	2.086	6.664	1.35	4.246
266.4	1.959	5.126	1.99	2.444×10^{-2}
264.4	1.840	3.946	2.32	3.413×10^{-3}

and 10 cm³ water with 650 g·m^{-3} SDS.[17] For comparison, the rate constant K was transformed into specific rate constant K' by simply using $K' = K/m_w$, where m_w is the mass of water.

Figure 8 shows the plots of ln K' vs $1/T$ of methane hydrate formed in three different media. The plots show good linear fits between ln K' and $1/T$ below ice point for all three cases, suggesting the following Arrhenius-type equation for K'

$$K' = K_0 \exp\left(-\frac{E_a}{RT}\right) \tag{8}$$

The values of K_0 and activation energy E_a were determined and are listed in Table 4.

As shown in Tables 1−3 and Figure 8, it is clear that the specific decomposition rate constant K' for hydrate in activated carbon is remarkably larger than that for bulk hydrate, with or without the presence of SDS. The larger K' in activated carbon than in a bulk free system should be mainly attributed to the much larger specific surface area of hydrate in porous activated carbon. As the hydrate formed in the presence of SDS is in the form of fine powder, its specific surface area is also bigger than that of hydrate formed in pure water, which leads to K' slightly larger in the presence of SDS than without the presence of SDS. From Table 4, it can be seen that the decomposition activation energy for hydrate in activated carbon below ice point is slightly lower than those for bulk free hydrates. This also implies that the decomposition of hydrate in porous activated carbon is easier than in bulk systems. The presence of SDS has little effect on the activation energy of decomposition. Compared with the activation energy for methane hydrate decomposition in structure I and structure II above ice point, 78.3 and 77.33 kJ/mol, respectively, determined by Kim et al.[11] and Clarke and Bishnoi,[14] hydrate decomposition below ice point requires higher activation energy.

As shown in Figure 8 and Table 4, the decomposition rate constant K' is weakly temperature dependent above ice point

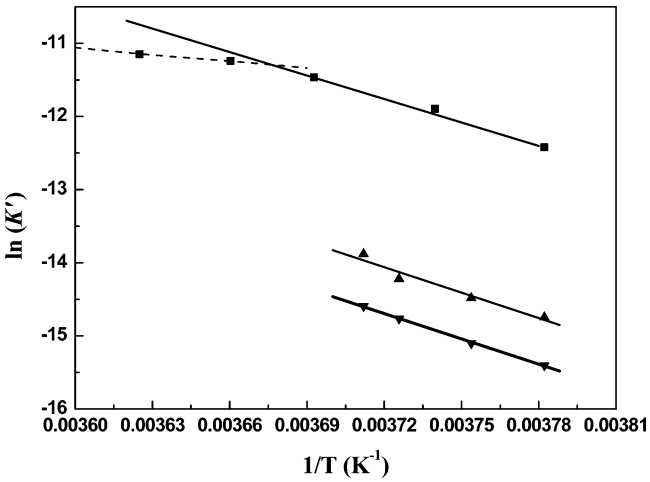

Figure 8. Arrhenius plot for methane hydrate decomposition: (■) hydrate formed in wet activated carbon; (▲) hydrate formed from 10 cm³ water with 650 g·m^{-3} SDS; (▼) hydrate formed from 10 cm³ pure water.

TABLE 4: The Value of K_0 and E_a in eq 8 Corresponding to Methane Hydrate Decomposition in Different Conditions

conditions for hydrate decomposition	$K_0 \times 10^{-12}$/ mol·MPa^{-1}·s^{-1}·g^{-1}	E_a/kJ·mol^{-1}
hydrate decomposed in activated carbon above ice point	1.22	26.03
hydrate decomposed in activated carbon below ice point	1.53×10^{12}	88.98
hydrate decomposed with the presence of 650 g·m^{-3} SDS	4.297×10^{12}	96.43
hydrate decomposed without the presence SDS	1.975×10^{12}	96.12

and the "activation energy" is only 26.03 kJ/mol, which is remarkably lower than 78.3 kJ/mol.[11] These results seems to be difficult to be accepted; however, they can be interpreted by the results recently reported by Stern et al.[30] in a study on the role of water in gas hydrate dissociation. The decomposition experiments of methane hydrate conducted within the anomalous preservation regime (240−270 K) by Stern et al.[15,22−23] demonstrated that there were no appreciable thermal differences between the interior of the hydrate sample and its surroundings (fluid bath). Although samples exhibited a brief temperature excursion resulting mainly from adiabatic cooling produced during the rapid depressurization, sample temperature then reequilibrates with external fluid bath temperature within several minutes; a very short duration compared with the time the decomposition test lasted. However, they observed that, when hydrate decomposed above ice point, there were large differences between sample temperature and fluid bath temperature; sample temperatures were buffered in a narrow temperature range below ice point that were independent of external bath temperature.[30] In that case, the dissociation rate was controlled by the rate of heat flow from the external bath as the intrinsic decomposition rate is essentially a constant. Therefore, the values of K in eq 7 determined by correlating formation rate data at fixed external bath temperatures above ice point should not be taken as the intrinsic decomposition rate constants at those external bath temperatures; the value of E_a, 26.03 kJ/mol, determined on their basis should not be taken as the real activation energy. That is to say, the model developed in this work, eq 7, is not physically suitable for the hydrate decomposition in a static system above ice, where the heat transfer is a control step.

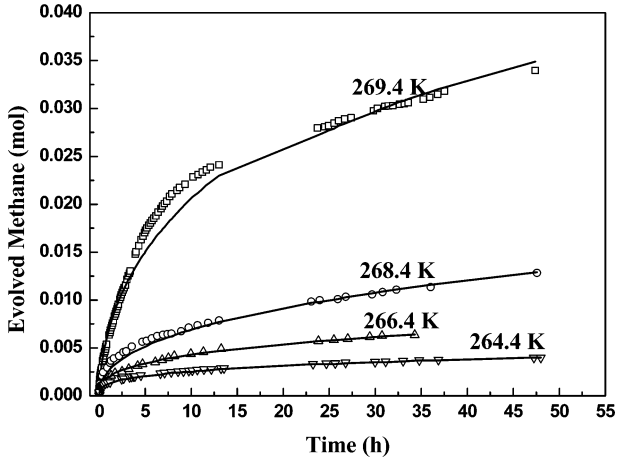

Figure 9. Cumulative moles of methane evolved at different times with respect to the dissociation of methane hydrate formed from 10 cm^3 pure water. The open symbols represent the experimental data. The solid curves are calculated from the model.

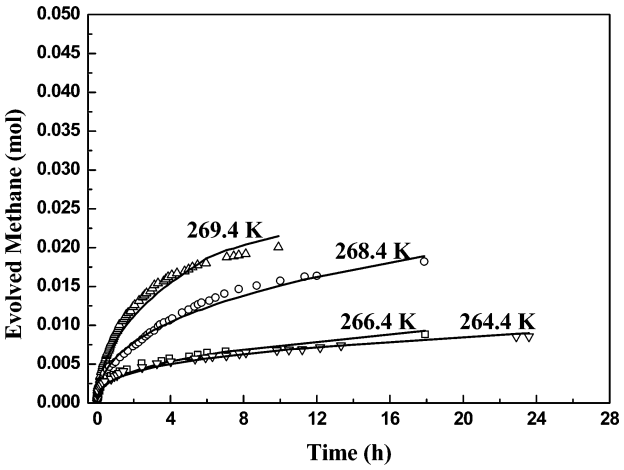

Figure 10. Profiles of cumulative moles of methane evolved at different temperatures with respect to the dissociation of methane hydrate formed from 10 cm^3 aqueous solution of 650 $g \cdot m^{-3}$ SDS. The open symbols represent the experimental data. The solid curves are calculated from the model.

The values of b with respect to the hydrate dissociation in activated carbon are also obviously bigger than those with respect to another two cases. The bigger value of b implies that the diffusion resistance increases more rapidly, the self-preservation effect is more obvious, and the dissociation of hydrate stopped sooner. It also implies that, only if K is small enough, hydrate should be more stable in porous activated carbon than in free systems. The presence of SDS essentially has no effect on the value of b. In all cases, parameter D_s is very sensitive to temperature. It decreases rapidly with the decrease of temperature and leads to an increase in self-preservation effect. Above the ice point, the values of D_s are 3−5 orders larger in magnitude than those below ice point, which implies a very small diffusion limitation.

The comparison of experimental data with calculated results by eq 7 were shown in Figure 3, Figure 9, and Figure 10. It can be seen that the agreement between the experimental data and the calculated results is satisfactory below ice point, especially at lower temperature range, while the agreement is relatively poor at temperatures near or above ice point. It again implies that the decomposition kinetic model developed in this work is not suitable for the decomposition above ice point.

5. Conclusions

The decomposition kinetic behaviors of methane hydrates formed in 5 cm^3 porous wet activated carbon were studied experimentally in a closed system in the temperature range of 275.8−264.4 K. The decomposition rates of methane hydrates formed from 5 cm^3 pure free water and an aqueous solution of 650 $g \cdot m^{-3}$ SDS were also measured for comparison. The experimental results manifested that both the decomposition rate of methane hydrate formed in 5 cm^3 wet activated carbon and that of methane hydrate formed from 5 cm^3 aqueous solution of SDS decreased monotonically with the decrease of the temperature. However, an abnormal phenomenon that hydrate dissociated much more rapidly at 264.4 K than at 267.4 K was observed in the decomposition of the hydrate formed from 5 cm^3 pure free water. The decomposition rates of methane hydrates in seven different cases were compared. The comparison showed that, except for the abnormal case observed in the decomposition of methane hydrate formed from 5 cm^3 pure free water, methane hydrate dissociated fastest in activated carbon, hydrate with a larger volume dissociated more slowly than that with a smaller volume, hydrate dissociated more slowly in a closed system than in an open system, and the presence of SDS increased the dissociation rates. A new mathematical model was developed to describe the decomposition kinetics of methane hydrates below ice point, in which the diffusion of methane molecules through the ice layer was assumed to be one of the control steps. By correlating experimental data, the parameters in the kinetic model were determined with respect to the decomposition of hydrates formed in the activated carbon, pure free water, and aqueous solution of SDS, respectively. It was demonstrated that the kinetic model satisfactorily describes the decomposition behavior of methane hydrate in different media.

Acknowledgment. The financial support received from the National Natural Science Foundation of China (nos. 20490207, 20176028, 90210020) and the Huo Yingdong Education Foundation (no. 81064) is gratefully acknowledged.

References and Notes

(1) Claussen, W. F. *J. Chem. Phys.* **1951**, *19*, 1425.
(2) von Stackelberg, M.; Müller, H. R. *Z. Electrochem.* **1954**, *58*, 25.
(3) Jeffery, G. A.; McMullan, R. K. *Prog. Inorg. Chem.* **1967**, *8*, 45.
(4) Ripmeester, J. A.; Ratcliffe, C. I.; Tse, J. S. *J. Chem. Soc., Faraday Trans.* **1988**, *84*, 3731.
(5) Gudmundsson, J. S.; Khokhar, A. A.; Parlaktuna, M. *Proceedings of the 67th Annual Technical Conference and Exhibition of SPE* **1990**, *SPE 24924*, 699.
(6) Yan, L. J.; Chen, G. J.; Pang, W. X.; Liu, J. *J. Phys. Chem. B* **2005**, *109*, 6025.
(7) Zhou, L.; Sun, Y.; Zhou, Y. *AIChE J.* **2002**, *48*, 2412.
(8) Perrin, A.; Celzard, A.; Marêché, J. F.; Furdin, G. *Carbon* **2004**, *42*, 1243.
(9) Zanota, M. L.; Perier-Camby, L.; Chauvy, F.; Brulle, Y.; Herri, J. M. *Proceedings of the 5th International Conference on Gas Hydrates*, Trondheim, Norway, **2005**, *4*, 1349.
(10) Suess, E.; Bohrmann, G.; Greinert, J.; Lausch, E. *Sci. Am.* **1999**, *281*, 76.
(11) Kim, H. C.; Bishnoi, P. R.; Heidemann, R. A.; Rizvi, S. S. H. *Chem. Eng. Sci.* **1987**, *42*, 1645.
(12) Clarke, M. A.; Bishnoi, P. R. *Chem. Eng. Sci.* **2000**, *55*, 4869.
(13) Clarke, M. A.; Bishnoi, P. R. *Can. J. Chem. Eng.* **2001**, *79*, 143.
(14) Clarke, M. A.; Bishnoi, P. R. *Chem. Eng. Sci.* **2001**, *56*, 4715.
(15) Stern, L. A.; Circone, S.; Kirby, S. H. *J. Phys. Chem. B* **2001**, *105*, 1756.
(16) Shirota, H.; Aya, I.; Namie, S. *Proceedings of the 4th International Conference on Gas Hydrates*, Yokohama, Japan **2002**, *2*, 972.
(17) Lin, W.; Chen, G. J.; Sun, C. Y.; Guo, X. Q.; Wu, Z. K.; Liang, M. Y.; Chen, L. T.; Yang, L. Y. *Chem. Eng. Sci.* **2004**, *59*, 4449.
(18) Yousif, M. H.; Sloan, E. D. *SPE Reservoir Eng.* **1991**, *6*, 69.
(19) Handa, Y. P.; Stupin, D. *J. Phys. Chem.* **1992**, *96*, 8599.

(20) Davidson, D. W.; Garg, S. K.; Gough, S. R.; Handa, Y. P.; Ratcliffe, C. I.; Ripmeester, J. A.; Tse, J. S.; Lawson, W. F. *Geochim. Cosmochim. Acta* **1986**, *50*, 619.

(21) Ershov, E. D.; Yakushev, V. S. *Cold Reg. Sci. Technol.* **1992**, *20*, 147.

(22) Stern, L. A.; Circone, S.; Kirby, S. H.; Durham, W. B. *Can. J. Phys.* **2003**, *81*, 271.

(23) Stern, L. A.; Circone, S.; Kirby, S. H.; Durham, W. B. *Proceedings of the 4th International Conference on Gas Hydrates*, Yokohama, Japan **2002**, *2*, 673.

(24) Stern, L. A.; Circone, S.; Kirby, S. H.; Durham, W. B. *J. Phys. Chem. B* **2002**, *106*, 228.

(25) Kuhs, W. F.; Genov, G.; Staykova, D. K.; Hansen, T. *Proceedings of the 5th International Conference on Gas Hydrates*, Trondheim, Norway **2005**, *1*, 14.

(26) Takeya, S.; Shimada, W.; Kamata, Y.; Ebinuma, T.; Uchida, T.; Nagao, J.; Narita, H. *J. Phys. Chem. A* **2001**, *105*, 9756.

(27) Genov, G.; Kuhs, W. F.; Staykova, D. K. *Proceedings of the 5th International Conference on Gas Hydrates*, Trondheim, Norway **2005**, *1*, 310.

(28) Tse, J. S.; Klug, D. D. *Proceedings of the 4th International Conference on Gas Hydrates*, Yokohama, Japan **2002**, *2*, 669.

(29) Wilder, J. W.; Smith, D. H. *J. Phys. Chem. B* **2002**, *106*, 226.

(30) Circone, S.; Stern, L. A.; Kirby, S. H. *J. Phys. Chem. B* **2004**, *108*, 5747.

(31) Peng, D. Y.; Robinson, D. B. *Ind. Chem. Fundam.* **1976**, *15*, 59.

(32) Sloan, E. D. *Clathrate Hydrates of Natural Gases*, 2nd ed.; Marcel Dekker: New York, 1998.

(33) Englezos, P.; Kalogerakis, N.; Dholabhai, P. D.; Bishnoi, P. R. *Chem. Eng. Sci.* **1987**, *42*, 2647.

(34) Melnilov, V.; Nesterov, A. *Proceeding of the 2nd International Conference on Natural Gas Hydrates*. Toulouse, France **1996**, 541.